

Algebraic charge liquids

Ribhu K. Kaul,¹ Yong Baek Kim,² Subir Sachdev,¹ and T. Senthil³

¹*Department of Physics, Harvard University, Cambridge MA 02138*

²*Department of Physics, University of Toronto, Toronto, Ontario M5S 1A7, Canada*

³*Department of Physics, Massachusetts Institute of Technology, Cambridge, Massachusetts 02139*

(Dated: June 2007)

High temperature superconductivity emerges in the cuprate compounds upon changing the electron density of an insulator in which the electron spins are antiferromagnetically ordered. A key characteristic of the superconductor [1] is that electrons can be extracted from them at zero energy only if their momenta take one of four specific values (the ‘nodal points’). A central enigma has been the evolution of the zero energy electrons in the metallic state between the antiferromagnet and the superconductor, and recent experiments yield apparently contradictory results. The oscillation of the resistance in this metal as a function of magnetic field [2, 3] indicate that the zero energy electrons carry momenta which lie on elliptical ‘Fermi pockets’, while ejection of electrons by high intensity light indicates that the zero energy electrons have momenta only along arc-like regions [4, 5]. We present a theory of new states of matter, which we call ‘algebraic charge liquids’, which arise naturally between the antiferromagnet and the superconductor, and reconcile these observations. Our theory also explains a puzzling dependence of the density of superconducting electrons on the total electron density, and makes a number of unique predictions for future experiments.

Soon after the discovery of high temperature superconductivity, Anderson [6] presented influential ideas on its connection to a novel type of insulator, in which the electron falls apart into emergent fractional particles which separately carry its spin and charge. These ideas have been extensively developed [7], and can explain the nodal zero-energy electron states in the superconductor. However, it is now known that the actual cuprate insulators are not of this type, and instead have conventional antiferromagnetic order, with the electron spins aligned in a checkerboard pattern on the square lattice. A separate set of ideas [8]

take the presence of antiferromagnetic order in the insulator seriously, but require a specific effort to induce zero energy nodal electrons in the superconductor.

Our theory of algebraic charge liquids (ACLs) uses the the recently developed theoretical framework of ‘deconfined quantum criticality’ [9] to describe the quantum fluctuations of the electrons. We show how this framework naturally combines the virtues of the earlier approaches: we begin with the antiferromagnetic insulator, but obtain electron fractionalization upon changing the electron density. A number of experimental observations in the so-called ‘underdoped’ region between the antiferromagnet and the superconductor also fall neatly into place.

A key characteristic of an ACL is the presence of an emergent fractional particle which carries charge e , no spin, and has Fermi statistics. We shall refer to this fermion as a ‘holon’. The holon comes in two species, carrying charges ± 1 in its interaction with an emergent gauge field a_μ , where μ is a spacetime index; this is a U(1) gauge field, similar to ordinary electromagnetism. However, the analog of the electromagnetic fine structure constant is of order unity for a_μ , and so its quantum fluctuations have much stronger effects. We also introduce operators f_\pm^\dagger which create holons with charges ± 1 . From the f_\pm and a_μ we can construct a variety of observables whose correlations decay with a power-law as function of distance or time in an ACL. These include valence-bond-solid and charge-density wave orders similar to those observed in recent scanning-tunnelling microscopy experiments [10].

While the f_\pm carry the charge of the electron in the ACL, the spin of the electron resides on another fractional particle, the ‘spinon’, with field operator z_α where $\alpha = \uparrow, \downarrow$ is the spin index. The spinon is electrically neutral, and also carries a_μ gauge charge. In an ACL, the spinon is simply related to the antiferromagnetic order parameter; if \hat{n} is the unit vector specifying the local orientation of the checkerboard spin ordering, then $\hat{n} = z^\dagger \vec{\sigma} z$, where $\vec{\sigma}$ are the Pauli matrices.

The nomenclature ‘ACL’ signals a formal connection to the previously studied *insulating* ‘algebraic spin liquids’ [9, 11, 12, 13, 14] which have power-law spin correlations, and of which the deconfined critical point is a particular example. However, the observable properties of the ACLs are completely different, with the ‘algebraic’ (or, equivalently ‘critical’) correlations residing in the charge sector.

We begin our more detailed presentation of the ACLs by first considering the simpler state in which long-range antiferromagnetic order is preserved, but a density x of electrons (per

Cu atom) have been removed from the insulator. This is the AF Metal of Fig. 1. This state has been extensively discussed and well understood in the literature, and its properties have been recently summarized in Ref. [15] using the same language we use here. Each missing electron creates a charge e , spin $S = 1/2$ fermionic ‘hole’ (to be distinguished from the spinless ‘holon’) in the antiferromagnetic state. It is known that the momenta of the holes reside in elliptical Fermi pockets centered at the points $K_i = (\pm\pi/2a, \pm\pi/2a)$ in the square lattice Brillouin zone (of lattice spacing a) - see Fig 2. This is a conventional metallic state, not an ACL, with hole-like zero energy excitations (or equivalently, the hole ‘Fermi surface’) along the dashed lines in Fig 2. In such a state, both the oscillations of the resistance as a function of applied magnetic field (SdH for Shubnikov-de Haas) *and* emission of electrons by light (ARPES for angle-resolved photoemission) would indicate zero energy electron states at the *same* momenta: along the dashed lines in Fig 2.

Now let us destroy the antiferromagnetic order by considering the vicinity of the deconfined critical point in the insulator [9]. Arguments were presented in Ref. [15] that we obtain a stable metallic state in which the electron fractionalizes into particles with precisely the quantum numbers of the f_{\pm} and the z_{α} described above. This is the holon metal phase: a similar phase was discussed in early work by Lee [16], but its full structure was clarified recently [15]. Below we will discuss the properties of the holon metal, and of a number of other ACLs that descend from it.

(i) Holon metal.

There is full spin rotation symmetry, and a positive energy (the spinon energy gap) is required to create a z_{α} spinon. The zero energy holons inherit the zero energy hole states of the AF Metal, and so they reside along the dashed elliptical pockets in Fig 2, and these will yield SdH oscillations characteristic of these pockets [17]. However, the view from ARPES experiments is very different—the distinction between SdH and ARPES views is a characteristic property of all ACLs. The physical electron is a composite of z_{α} and f_{\pm} , and so the ARPES spectrum will have no zero energy states, and only a broad absorption above the spinon energy gap. The frequency F of the SdH oscillations is given by the Onsager-Lifshitz relation

$$F = \Phi_0 \mathcal{A} / (2\pi^2), \quad (1)$$

where $\Phi_0 = hc/(2e)$ is the flux quantum, and \mathcal{A} is the area in momentum space enclosed

by the fermionic zero-energy charge carriers. For the holons, this area is specified by the Luttinger relation: there are 4 independent holon pockets, and the area of each pocket is

$$\mathcal{A}_{\text{holon}} = (2\pi)^2 x / (4a^2). \quad (2)$$

(ii) Holon-hole metal

This is our candidate state for the normal state of the cuprates at low hole density (see Fig 1). It is obtained from the holon metal when some of the holons and spinons bind to form a charge e , $S = 1/2$ particle, which is, of course, the conventional hole, neutral under the a_μ charge. This binding is caused by the nearest-neighbor electron hopping, and the computation of the dispersion of the bound state is described in the Appendix. Now the metal has both holons and hole charge carriers, and both have independent zero energy states, *i.e.* Fermi surfaces. These Fermi surfaces are shown in Fig. 2, and *both* enclosed areas will contribute a SdH frequency via Eq. (1). The values of the areas depend upon specific parameter values, but the Luttinger relation does yield the single constraint

$$\mathcal{A}_{\text{holon}} + 2\mathcal{A}_{\text{hole}} = (2\pi)^2 x / (4a^2); \quad (3)$$

the factor of 2 prefactor of $\mathcal{A}_{\text{hole}}$ is due to $S = 1/2$ spin of the holes. This relation can offer an explanation of the recent experiment [2] which observed SdH oscillations at a frequency of $530T$. We propose that these oscillations are due to the holon states. The holon density may then be inferred to be 0.076 per Cu site while the total doping is $x = 0.1$. The missing density resides in the hole pockets, which by Eq. (3) will also exhibit oscillations at the frequency associated with the area $[(2\pi)^2 / (4a^2)] \times 0.012$. The presence of SdH oscillations at this lower frequency is a key prediction of our theory which we hope will be tested experimentally. ARPES experiments detect only the hole Fermi surface, *i.e.* the ‘bananas’ in Fig. 2. With a finite momentum width due to impurity scattering, and the very small area of each banana, the holon-hole metal also accounts for the arc-like regions observed in current ARPES experiments [1, 4, 5]. Furthermore, because the nearest neighbor electron hopping is suppressed by local antiferromagnetic correlations, we expect the binding to increase with temperature, and this possibly accounts for the observed temperature dependence of the arcs [5, 15].

(iii) Holon superconductor.

Upon lowering the temperature in the holon metal, the holons pair to form a composite boson which is neutral under the a_μ charge, and the condensation of this boson leads to the holon superconductor. Just as we determined the holon dispersion in the holon metal phase by referring to previous work in the proximate AF metal, we can determine the nature of the pair wavefunction by extrapolating from the state with co-existing antiferromagnetism and superconductivity in Fig 1. The latter state was studied by Sushkov and collaborators [18, 19], and they found that holes paired with d -wave symmetry. Hence the AF+dSC state in Fig 1. We assume that the same pairing amplitude extends into the ACL obtained by restoring spin rotation symmetry and inducing a spinon energy gap. The resulting holon superconductor is not smoothly connected to the conventional BCS d -wave superconductor because of the spin gap. The theory describing the low energy excitations of the holons in the holon superconductor is developed in the Appendix: it is found to be a mathematical structure known as a conformal field theory (CFT). The present CFT has the U(1) gauge field a_μ coupled minimally to $N = 4$ species of Dirac fermions, ψ_i ($i = 1 \dots N$), which are descended from the f_\pm holons after pairing. Such CFTs have been well-studied in other contexts [11, 12, 13, 20]. For us, the important utility of the CFT is that it allows us to compute the temperature (T) and x dependence of the density of superfluid electron, ρ_s (measured in units of energy through its relation to the London penetration depth, λ_L by $\rho_s = \hbar^2 c^2 d / (16\pi e^2 \lambda_L^2)$, with d the spacing between the layers in the cuprates). For this, we need the coupling of the CFT to the vector potential \vec{A} of the electromagnetic field: this is studied in the Appendix and has the form $\vec{j} \cdot \vec{A}$ where \vec{j} is a conserved ‘flavor’ current of the Dirac fermions ψ_i . The T dependence of ρ_s is then related to the T dependence of the susceptibility associated with \vec{j} : such susceptibilities were computed in Ref. [21]. In a similar manner we found that as $T \rightarrow 0$ at small x

$$\rho_s(x, T) = c_1 x - \mathcal{R} k_B T \quad (4)$$

where c_1 is a non-universal constant and \mathcal{R} is a universal number characteristic of CFT. Remarkably, such a ρ_s is seen in experiments [22, 23, 24] on the cuprates over a range of T and x . The phenomenological importance of such a $\rho_s(x, T)$ was pointed out by Lee and Wen [26], although Eq. (4) has not been obtained in any earlier theory [27]. The holon superconductor provides an elegant route to this behavior, moreover with \mathcal{R} universal. We

analyzed the CFT in a $1/N$ expansion and obtained

$$\mathcal{R} = 0.4412 + 0.074/N. \quad (5)$$

We note that in the cuprates, there is a superconductor-insulator transition at a non-zero $x = x_c$, and in its immediate vicinity distinct quantum critical behavior of ρ_s is expected, as has been observed recently[25]. However, in characterizing different theories of the underdoped regime, it is useful to consider the behavior as $x \rightarrow 0$ assuming the superconductivity survives until $x = 0$. In this limit, our present theory is characterized by $d\rho_s/dT \sim \text{constant}$, while theories of Refs. [27, 28] have $d\rho_s/dT \sim x^2$.

(iv) **Holon-hole superconductor.**

This is our candidate state of the superconductor at low hole density (see Fig 1). It is obtained from a pairing instability of the holon-hole metal, just as the holon superconductor was obtained from the holon metal. It is a modified version of the holon superconductor, which has in addition low energy excitations from the paired holes. The latter will yield the observed V-shaped spectrum in tunneling measurements. The holon-hole metal will also have a residual metallic thermal conductivity at low T in agreement with experiment. For $\rho_s(x, T)$ we will obtain in addition to the terms in Eq. (4), a contribution from the nodal holes to $d\rho_s/dT$. This contribution can be computed using the considerations presented in Refs. [26, 27]: it has only a weak x -dependence coming from the ratio of the velocities (which can in principle be extracted from ARPES) in the two spatial directions. In particular, the holes carry a current ~ 1 and not $\sim x$; the latter is the case in other theories [27, 28] of electron fractionalization which consequently have $d\rho_s/dT \sim x^2$.

Perhaps the most dramatic implication of these ideas is the possibility that the superconducting ground state of the underdoped cuprates is not smoothly connected to the conventional superconductors described by the theory of Bardeen, Cooper, and Schrieffer(BCS). With the reasonable additional assumption that such a BCS ground state is realized in the overdoped cuprates, it follows that our proposal requires at least one quantum phase transition *inside* the superconducting dome.

Correspondence and request for materials to T. Senthil (senthil@mit.edu). We thank Eric Hudson, Alessandra Lanzara, Patrick Lee, Mohit Randeria, Louis Taillefer, Ziqiang Wang, Zheng-Yu Weng, and Xingjiang Zhou for many useful discussions. This research

was supported by the NSF grants DMR-0537077 (SS and RKK), DMR-0132874 (RKK), DMR-0541988 (RKK), the NSERC (YBK), and the CIFAR (YBK).

APPENDIX

EFFECTIVE ACTION FOR HOLON METAL

We use the formulation in Ref. [15]. We represent the electron operator on square lattice site r and spin $\alpha = \uparrow, \downarrow$ as

$$c_{r\alpha} \sim f_r^\dagger z_{r\alpha} \quad r \in A \quad (6)$$

$$\sim \varepsilon_{\alpha\beta} f_r^\dagger z_{r\beta}^* \quad r \in B \quad (7)$$

where A, B are the 2 sublattices, and $\varepsilon_{\alpha\beta}$ is the unit antisymmetric tensor. The f_r are spinless charge- e fermions that carry opposite a_μ gauge charge ± 1 on the 2 sublattices. They will be denoted f_\pm respectively. The effective action of the doped antiferromagnet on the square lattice has the structure

$$\begin{aligned} \mathcal{S} &= \mathcal{S}_z + \mathcal{S}_f + \mathcal{S}_t \\ \mathcal{S}_z &= \int d\tau \sum_r \frac{1}{g} |\partial_\tau z|^2 - \sum_{\langle rr' \rangle} \frac{1}{g'} (z_r^* z_{r'} + \text{c.c.}) \\ \mathcal{S}_f &= \int d\tau \sum_{s=\pm} \sum_K f_s^\dagger(K) (\partial_\tau + \epsilon_K - \mu_h) f_s(K) \\ \mathcal{S}_t &= \int d\tau \kappa_0 \sum_r c_r^\dagger c_r - \kappa \sum_{\langle rr' \rangle} c_r^\dagger c_{r'} + \text{c.c.}, \end{aligned} \quad (8)$$

where K is a momentum extending over the diamond Brillouin zone in Fig. 2. \mathcal{S}_z is the lattice action for the spinons, and we are interested here in the paramagnets obtained for large g, g' . \mathcal{S}_f describes the hopping of the holons on the same sublattice, preserving the sublattice index $s = \pm 1$; the holon dispersion ϵ_K has minima at the K_i , and μ_h is the holon chemical potential. The first term in \mathcal{S}_t describes an on-site electron chemical potential. The second corresponds to opposite sublattice electron hopping which we have taken to be between nearest neighbors; the coupling κ is expected to be significantly renormalized down by the local antiferromagnetic order [29] from the bare electron hopping element t . We have not included the a_μ gauge field in the above action; however, it is easily inserted by the

requirements of gauge invariance and minimal coupling to z with charge 1, and f_s which carries charge s [15].

For small g, g' , the z_α condense, and we obtain the familiar AF Metal state with hole pockets (see Fig. 1). In this phase, the f_\pm have the same quantum numbers as the hole *i.e.* they are $S = 1/2$ charge e quasiparticles [15]. For larger g, g' we reach the holon metal phase [15], in which the z are gapped. We first describe this phase while ignoring the κ term. Then the holons are free and form Fermi pockets centered at K_i . As the sublattice index s is conserved in the absence of the κ term the holons hop on just one sublattice. The appropriate Brillouin zone is therefore the diamond shaped one shown in Fig 2. However, it is important to note that this Brillouin zone is only significant in counting the degrees of freedom which carry gauge charges in this fractionalized phase; the diamond zone has no significance for gauge-invariant observables, and the full symmetry of the square lattice is preserved in the holon metal phase [15]. The stability of the holon metal towards a_μ gauge fluctuations was also discussed earlier [15]: the a_μ photon is strongly damped by its coupling to the holon Fermi surface, and monopoles in a_μ are also suppressed by this Fermi surface [12].

The S_t term (ignored so far) leads to two distinct (but not exclusive) instabilities of the holon metal phase: towards pairing of the f_\pm holons and the formation of bound states between the holons and spinons. These instabilities lead, respectively, to the holon superconductor and the holon-hole metal (and to holon-hole superconductor when both are present). We will consider these in the following sections.

We note in passing that the S_t term will also significantly modify the spin correlation spectrum, likely inducing incommensurate spin correlations [30], but this we will not address here.

HOLON SUPERCONDUCTOR

Consider, first, the pairing instability. In the phase with Néel order $\langle \hat{n} \rangle \neq 0$, this κ -induced pairing was studied in some detail [18, 19] in a model essentially equivalent to ours. We assume here the pairing signature found by them persists into the holon metal phase with $\langle \hat{n} \rangle = 0$, which is reasonable as long as there are short-range Néel correlations. The pairing is between opposite gauge charges, $\langle f_+^\dagger f_-^\dagger \rangle \neq 0$, and so is assisted by the attractive a_μ

gauge force. This order parameter carries physical charge $2e$, spin 0, and gauge charge 0. To describe the pairing, we first separate the holon dispersion in Eq. (8) into four separate valleys which lie within the i 'th quadrant of the diamond Brillouin zone, and measure momenta, $k = K - Q_i$, for the respective valleys from the points $Q_i = (\pm Q, \pm Q)$ where the holon Fermi surfaces cross the diagonal directions (see Fig. 2). We now have fermions $f_{is}(k)$, where i is a valley index, with the dispersion

$$\mathcal{H}_{\text{holon metal}} = \sum_{s=\pm} \sum_{i=1}^4 \sum_k \epsilon_{ik} f_{is}^\dagger(k) f_{is}(k) \quad (9)$$

where for small $|k|$

$$\epsilon_{1k} = -\frac{v_F}{\sqrt{2}}(k_x + k_y) \quad , \quad \epsilon_{2k} = \frac{v_F}{\sqrt{2}}(k_x - k_y)$$

and $\epsilon_{3k} = -\epsilon_{1k}$, $\epsilon_{4k} = -\epsilon_{2k}$. Here v_F is the holon Fermi velocity. The pairing found in Refs. [18, 19] has a p -wave signature for the f_{is} holons, and was shown to correspond to $d_{x^2-y^2}$ pairing for the physical electrons. In our notation, the pairing amplitudes are

$$\begin{aligned} \Delta_1(k) &= \langle f_{+1}^\dagger(k) f_{-3}^\dagger(-k) \rangle = \frac{v_\Delta}{\sqrt{2}}(k_x - k_y) \\ \Delta_2(k) &= \langle f_{+2}^\dagger(k) f_{-4}^\dagger(-k) \rangle = -\frac{v_\Delta}{\sqrt{2}}(k_x + k_y) \end{aligned} \quad (10)$$

and similarly for $\Delta_{3,4}$, and it was found that $v_\Delta \sim v_F$ [18]. Note that the a_μ gauge symmetry remains unbroken even upon the onset of pairing. We can now write Eqs. (9-10) in real space, reinsert the coupling to the a_μ , and obtain a CFT for the holon superconductor in a series of familiar steps: we introduce the Nambu spinors $\chi_i = (f_{i+}, f_{\bar{i}-}^\dagger)$ (where \bar{i} is the valley antipodal to i) and Pauli matrices $\vec{\tau}$ in Nambu space, define four Dirac fermions ψ_i by $\chi_1 = e^{-i\pi\tau^y/4}\tau^x\psi_1$, $\chi_2 = \tau^y\psi_2$, $\chi_3 = e^{-i\pi\tau^y/4}\tau^z\psi_3$, $\chi_4 = \psi_4$, rotate the spatial co-ordinate system by a $\pi/4$ angle to $R = (X, Y)$, and set $v_\Delta = v_F$ (this condition is achieved upon renormalization with a_μ fluctuations [13, 20]). This yields

$$\begin{aligned} \mathcal{S}_{\text{holon superconductor}} &= \int d\tau d^2R \left[\frac{1}{2e_0^2} (\epsilon_{\mu\nu\lambda} \partial_\nu a_\lambda)^2 \right. \\ &\quad \left. + \sum_{i=1}^4 \psi_i^\dagger (D_\tau - iv_F D_X \tau^x - iv_F D_Y \tau^z) \psi_i \right] \end{aligned} \quad (11)$$

Here μ, ν, λ, \dots are spacetime indices (τ, X, Y) , and $D_\mu = \partial_\mu - ia_\mu$. This action describes massless QED₃ theory with $N = 4$ species of 2-component Dirac fermions. Within the $1/N$

expansion, it is known to flow at low energies to a stable fixed point [11, 12] describing a CFT.

We now compute the superfluid density, $\rho_s(x, T)$. As the superconductivity arises through pairing of holons from a Fermi surface of area $\propto x$, we have $\rho_s(x, 0) \propto x$. At $T > 0$ we need to include thermal excitation of unpaired holons, which are coupled to the vector potential \vec{A} of the physical electromagnetism by

$$\mathcal{H}_A = \sum_{is} \sum_k \vec{A} \cdot \frac{\partial \epsilon_{ki}}{\partial \vec{k}} f_{iks}^\dagger f_{iks} \equiv \vec{j} \cdot \vec{A}$$

In terms of the Dirac fermions

$$j_X = v_F \left(\psi_3^\dagger \psi_3 - \psi_1^\dagger \psi_1 \right) \quad , \quad j_Y = v_F \left(\psi_4^\dagger \psi_4 - \psi_2^\dagger \psi_2 \right) ,$$

which are *conserved* ‘‘charges’’ of Eq. (11). The susceptibility associated with these charges is $\propto T$ [21], and so we obtain the Eq. (4)

$$\rho_s(x, T) = c_1 x - \mathcal{R} k_B T \tag{12}$$

where c_1 is a non-universal constant and \mathcal{R} is a universal number characteristic of CFT. Other low T properties of the holon superconductor are similar to an ordinary BCS d -wave superconductor with normal nodal quasiparticles: the low- T specific heat (including the Volovik term in a magnetic field) and metallic heat conduction.

HOLON-SPINON BINDING

Finally, we consider the κ -induced holon-spinon binding in the holon metal which leads to the appearance of the holon-hole metal at low temperatures. Similar methods apply to holon superconductor, where the binding leads to the holon-hole superconductor.

It is evident from Eq. (8) that \mathcal{S}_t is an attractive interaction between the z and the f . Moreover, the attraction is strongly momentum dependent: as we will show below, for a holon-spinon pair with center-of-mass momentum K , there is a contact attractive potential proportional to $\kappa_0 - \kappa \gamma_K$, with $\gamma_K = (\cos(K_x) + \cos(K_y))$. Near the Brillouin zone edges where γ_K is small, the binding energy may be taken to have the form $V_0 - V_1 \gamma_K$, and this structure determines the ‘banana’ Fermi surfaces in Fig. 2.

We discuss the energy of a holon-spinon composite using a non-relativistic Schrodinger equation. For the time being we assume that

- (i) only a single holon is injected into the paramagnet
- (ii) all gauge interactions can be ignored.

Both these assumptions will be relaxed once the ‘mean field’ dispersion of the holons and the holon-spinon composites are determined.

We want to study bound holon-spinon composites associated with a single holon valley (say valley 1). For simplicity we also assume that the holon dispersion near \vec{K}_1 can be taken to be an isotropic parabola

$$E_f(\vec{k}) = \frac{k^2}{2m_h} \quad (13)$$

with $\vec{k} = \vec{K} - \vec{K}_1$, and that the spinon dispersion is

$$E_s(\vec{k}) = \Delta_s + \frac{k^2}{2\Delta_s} \quad (14)$$

Note that the spinon dispersion is centered at $(0, 0)$.

The energy of the holon-spinon composite will be

$$E_h(\vec{k}) = \frac{k^2}{2M} + \Delta_s - E_{\text{bind}}(\vec{k}) \quad (15)$$

where $M = m_h + \Delta_s$. The binding energy E_{bind} comes from \mathcal{S}_t and will be \vec{k} -dependent. This can be determined by solving a non-relativistic Schrodinger equation for the relative coordinate between the holon and spinon (similar to Section IV of Ref. [15]). Specifically, let $\phi_+(\vec{r}), \phi_-(\vec{r})$ be the wavefunctions of a composite of a \pm -holon and a spinon separated by \vec{r} and with center-of-mass momentum \vec{k} . Define

$$\phi(\vec{r}) = \begin{bmatrix} \phi_+(\vec{r}) \\ \phi_-(\vec{r}) \end{bmatrix}. \quad (16)$$

This satisfies the Schrodinger equation

$$\left(-\frac{\nabla^2}{2\rho} - (\kappa_0 - \kappa\sigma^x\tilde{\gamma}(k))\delta^2(\vec{r}) \right) \phi = -E_{\text{bind}}\phi \quad (17)$$

where $\rho = m_h\Delta_s/(m_h + \Delta_s)$ and $\tilde{\gamma}(k) = \gamma(\vec{K}_1 + \vec{k}) = -(\sin k_x + \sin k_y)$. The σ^x is a Pauli matrix that acts on ϕ . Clearly it is better to work with

$$\phi_{1,3} = \frac{\phi_+ \pm \phi_-}{\sqrt{2}} \quad (18)$$

The resulting Schrodinger equation then gives some binding energy

$$E_{\text{bind}}^{(1)} = E_{\text{bind}}^{(1)}(\kappa_0 - \kappa\tilde{\gamma}(\vec{k})) \quad (19)$$

$$E_{\text{bind}}^{(3)} = E_{\text{bind}}^{(3)}(\kappa_0 + \kappa\tilde{\gamma}(\vec{k})) \quad (20)$$

Focusing on hole $h_1 \sim \psi_1^\dagger$ the binding energy is largest when $\kappa_0 - \kappa\tilde{\gamma}(\vec{k})$ is as big as possible. For the momenta of interest, the $\tilde{\gamma}$ term is small and so we may approximate

$$E_{\text{bind}}^{(1)} \approx V_0 - V_1\tilde{\gamma}(\vec{k}) \quad (21)$$

with $V_0, V_1 > 0$. Thus the dispersion for h_1 becomes

$$E_{h_1}(\vec{k}) = \frac{k^2}{2M} + \Delta_s - V_0 + V_1\tilde{\gamma}(\vec{k}) \quad (22)$$

Consider this dispersion together with that of a single unbound holon. The minimum of E_{h_1} is at a non-zero energy. Further as a function of $k_X = (k_x + k_y)/2$ it is shifted along the positive k_X direction by an amount $2MV_1 \cos(k_Y)$ with $k_Y = (-k_x + k_y)/2$.

If we now start filling up these bands we see that at low doping only the holon bands will be occupied. However with increasing doping the hole band will also be occupied to get a holon-hole metal. In the full Brillouin zone h_1 is at momentum $-\vec{K}_1$ so that the hole Fermi surface lies entirely inside the diamond region. Further we see that the hole Fermi surface has the rough banana shape shown in Fig. 2. The gauge interaction can now be included and leads to the properties discussed in the main text.

-
- [1] A. Damascelli, Z. Hussain, and Z.-X. Shen, *Angle-resolved photoemission studies of the cuprate superconductors*, *Rev. Mod. Phys.* **75**, 473-541 (2003).
 - [2] N. Doiron-Leyraud *et al.*, *Quantum oscillations and the Fermi surface in an underdoped high- T_c superconductor*, *Nature* **447**, 565-568 (2007).
 - [3] E. A. Yelland *et al.*, *Quantum Oscillations in the Underdoped Cuprate YBa2Cu4O8*, arXiv:0707.0057.
 - [4] M. R. Norman *et al.*, *Destruction of the Fermi surface underdoped high- T_c superconductors*, *Nature* **392**, 157-160 (1998).
 - [5] A. Kanigel *et al.*, *Evolution of the pseudogap from Fermi arcs to the nodal liquid*, *Nature Physics* **2**, 447-451 (2006).
 - [6] P. W. Anderson, *The Resonating Valence Bond State in La2CuO4 and Superconductivity*, *Science* **235**, 1196-1198 (1987).
 - [7] P. A. Lee, N. Nagaosa, and X.-G. Wen, *Doping a Mott insulator: Physics of high-temperature superconductivity*, *Rev. Mod. Phys.* **78**, 17-86 (2006).

- [8] S. A. Kivelson *et al.*, *How to detect fluctuating stripes in the high-temperature superconductors*, *Rev. Mod. Phys.* **75**, 1201-1241 (2003).
- [9] T. Senthil *et al.*, *Deconfined quantum critical points*, *Science* **303**, 1490-1494 (2004).
- [10] Y. Kohsaka *et al.*, *An Intrinsic Bond-Centered Electronic Glass with Unidirectional Domains in Underdoped Cuprates*, *Science* **315**, 1380-1385 (2007).
- [11] W. Rantner and X.-G. Wen, *Electron spectral function and algebraic spin liquid for the normal state of underdoped high T_c superconductors*, *Phys. Rev. Lett.* **86**, 3871-3874 (2001).
- [12] M. Hermele *et al.*, *Stability of U(1) spin liquids in two dimensions*, *Phys. Rev. B* **70**, 214437 (2004).
- [13] M. Hermele, T. Senthil, and M. P. A. Fisher, *Algebraic spin liquid as the mother of many competing orders*, *Phys. Rev. B* **72** 104404 (2005).
- [14] B. L. Altshuler, L. B. Ioffe, and A. J. Millis, *Low-energy properties of fermions with singular interactions*, *Phys. Rev. B* **50** 14048-14064 (1994).
- [15] R. K. Kaul *et al.*, *Hole dynamics in an antiferromagnet across a deconfined quantum critical point*, *Phys. Rev. B* **75**, 235122 (2007).
- [16] P. A. Lee, *Gauge field, Aharonov-Bohm flux, and high- T_c superconductivity*, *Phys. Rev. Lett.* **63**, 680-683 (1989).
- [17] Y. B. Kim, P. A. Lee, and X.-G. Wen, *Quantum Boltzmann equation of composite fermions interacting with a gauge field*, *Phys. Rev. B* **52**, 17275-17292 (1995).
- [18] V. V. Flambaum, M. Yu. Kuchiev, and O. P. Sushkov, *Hole-Hole superconducting pairing in the t - J model induced by long-range spin-wave exchange*, *Physica C* **227**, 267-278 (1994).
- [19] V. I. Belinicher *et al.*, *Hole-Hole superconducting pairing in the t - J model induced by spin-wave exchange*, *Phys. Rev. B* **51**, 6076-6084 (1995).
- [20] O. Vafek, Z. Tesanovic, and M. Franz, *Relativity restored: Dirac anisotropy in QED₃*, *Phys. Rev. Lett.* **89**, 157003 (2002).
- [21] A. V. Chubukov, S. Sachdev, and J. Ye, *Theory of two-dimensional quantum Heisenberg antiferromagnets with a nearly critical ground state*, *Phys. Rev. B* **49**, 11919-11961 (1994).
- [22] D. A. Bonn *et al.*, *Surface impedance studies of YBCO*, *Czech. J. Phys.* **46**, 3195-3202 (1996).
- [23] B R. Boyce, J. Skinta, and T. Lemberger, *Effect of the pseudogap on the temperature dependence of the magnetic penetration depth in YBCO films*, *Physica C* **341-348**, 561 (2000).
- [24] M. Le Tacon *et al.*, *Two Energy Scales and two Quasiparticle Dynamics in the Superconducting*

- State of Underdoped Cuprates*, *Nature Physics* **2**, 537-543 (2006).
- [25] I. Hetel, T. R. Lemberger, and M. Randeria, *Quantum critical behaviour in the superfluid density of strongly underdoped ultrathin copper oxide films*, *Nature Physics* online, doi:10.1038/nphys707.
- [26] P. A. Lee and X.-G. Wen, *Unusual superconducting state of underdoped cuprates*, *Phys. Rev. Lett.* **78**, 4111-4114 (1997).
- [27] C. P. Nave, D. A. Ivanov, and P. A. Lee, *Variational Monte Carlo study of the current carried by a quasiparticle*, *Phys. Rev. B* **73**, 104502 (2006).
- [28] P. W. Anderson *et al.*, *The Physics Behind High-Temperature Superconducting Cuprates: The "Plain Vanilla" Version Of RVB*, *J Phys. Condens. Matter* **16**, R755-R769 (2004).
- [29] C. Kane, P.A. Lee, and N. Read, *Motion of a single hole in a quantum antiferromagnet*, *Phys. Rev. B* **39**, 6880 (1989).
- [30] B. I. Shraiman and E. D. Siggia, *Mobile Vacancies in a Quantum Heisenberg Antiferromagnet*, *Phys. Rev. Lett.* **61**, 467 (1988).

Figure Captions

1. **Schematic phase diagram at small x .** Here T is the temperature, and x is the density of electrons (per Cu atom) which have been removed from the insulator. The phases labelled “AF” have long-range antiferromagnetic order. The AF+dSC state also has d -wave superconductivity and was described in Ref. [18, 19]. For the cuprates, we propose that the ACL phase above is a holon-hole metal, while the superconducting ACL is the holon-hole superconductor. The conventional Fermi liquid metal and BCS superconductor appear at larger x , and are not shown.

2. **Square lattice Brillouin zone containing the ‘diamond’ Brillouin zone (dashed line).** In the AF Metal, only the dashed ellipses are present, and they represent Fermi surfaces of $S = 1/2$, charge e holes which are visible in both ARPES and SdH. In the holon metal, these dashed ellipses become spinless charge e holon Fermi surfaces, and are visible only in SdH. The full line ‘bananas’ are the hole Fermi surfaces present only in the holon-hole metal, and detectable in both SdH and ARPES.

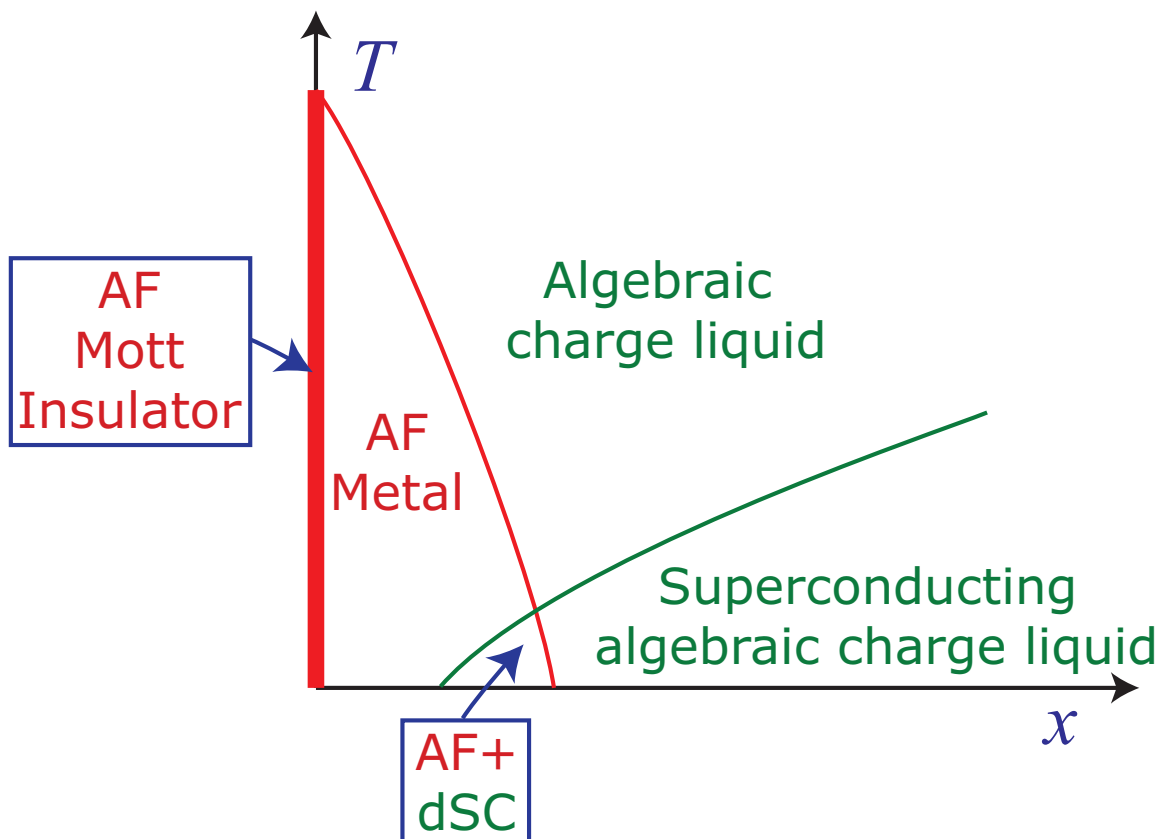


FIG. 1:

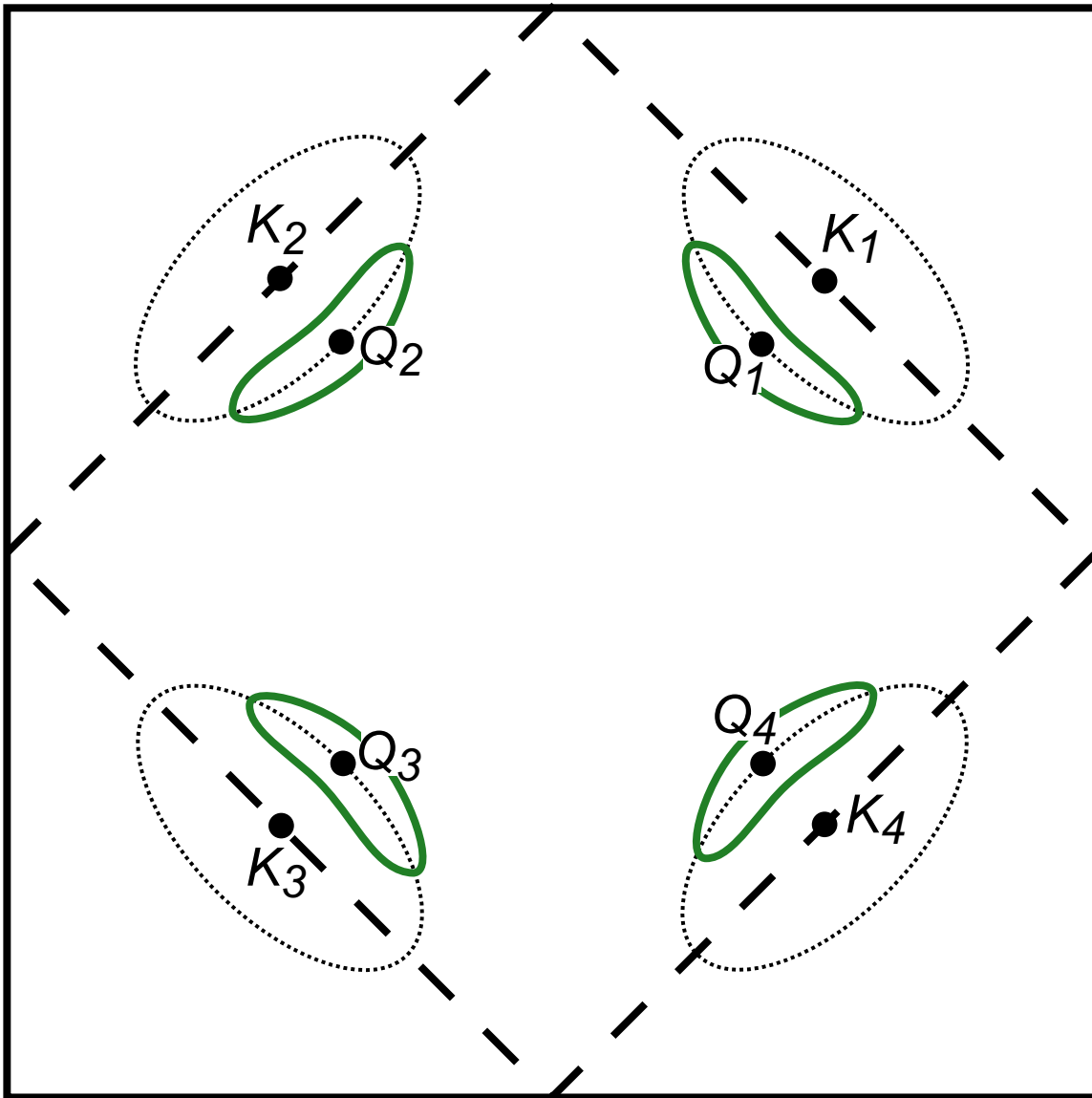


FIG. 2: